

1 **Damaging sediment density flows triggered by tropical cyclones**

2 Ed L. Pope^{1,2*}, Peter J. Talling^{1,3}, Lionel Carter⁴, Michael A. Clare¹, James E. Hunt¹

3 ¹*National Oceanography Centre, University of Southampton Waterfront Campus, European Way,*
4 *Southampton, SO14 3ZH, UK.*

5 ²*Department of Geography, Durham University, Science Laboratories, South Road, Durham, DH1 3LE,*
6 *UK.*

7 ³*Departments of Earth Science and Geography, Durham University, Science Laboratories, South Road,*
8 *Durham, DH1 3LE, UK.*

9 ⁴*Antarctic Research Centre, Victoria University of Wellington, Wellington, New Zealand.*

10 **Abstract**

11 The global network of subsea fibre-optic cables plays a critical role in the world economy and is
12 considered as strategic infrastructure for many nations. Sediment density flows have caused
13 significant disruption to this network in the recent past. These cable breaks represent the only
14 means to actively monitor such flows over large oceanic regions. Here, we use a global cable break
15 database to analyse tropical cyclone triggering of sediment density flows worldwide over 25 years.
16 Cable breaking sediment density flows are triggered in nearly all areas exposed to tropical cyclones
17 but most occur in the NW Pacific. They are triggered by one of three sets of mechanisms. Tropical
18 cyclones directly trigger flows, synchronous to their passage, as a consequence of storm waves,
19 currents and surges. Cyclones also trigger flows indirectly, with near-synchronous timing to their
20 passage, as a consequence peak flood discharges. Last, cyclones trigger flows after a delay of days as
21 a consequence of the failure of large volumes of rapidly deposited sediment. No clear relationship
22 emerges between tropical cyclone activity (i.e. track, frequency and intensity) and the number of
23 sediment density flows triggered. This is a consequence of the short period of observation. However,

24 expansion of the cable network and predicted changes to cyclone activity in specific regions
25 increases the likelihood of increasing numbers of damaging flows.

26 **Keywords**

27 Sediment density flows; cable breaks; tropical cyclones; climate change; hazards

28 *Corresponding Author – Ed.Pope@noc.soton.ac.uk

29 **1. Introduction**

30 Tropical cyclones are common in many regions of the world and affect nearly all tropical areas
31 (Emanuel, 2005). Associated with these meteorological phenomena are extreme winds, torrential
32 rains and subsequent river floods, increased surface run-off and/or landslides, large waves and
33 damaging storm surges leading to coastal flooding (Peduzzi et al., 2012). An often unrecognised
34 hazard is that posed to subsea infrastructure by cyclone-triggered sediment density flows.

35 Sediment density flows (a generic term used here to encompass turbidity currents, debris flows,
36 hyperpycnal plumes and submarine landslides, etc.) can travel at speeds of up to 19 ms^{-1} and runout
37 for several hundreds of kilometres. These flows can damage critical seafloor infrastructure, such as
38 that associated with the offshore hydrocarbon industry or subsea telecommunication cable
39 networks (Carter et al., 2009; Pope et al., 2016). The seafloor telecommunication network currently
40 carries >95% of global data and internet traffic making it integral to the global economy and
41 strategic infrastructure for many countries (Carter et al., 2009; Burnett et al., 2013). Determining the
42 timing and triggering of these flows is important for submarine geohazard assessment, especially
43 whether their frequency may change as the oceans warm due to predicted climate change (Stocker,
44 2014).

45 Multiple triggering mechanisms have been identified for sediment density flows. These include
46 earthquakes, tsunamis and storm wave loading, rapid sediment deposition and oversteepening,

47 direct plunging of dense river water (hyperpycnal flows) and volcanic activity (Piper and Normark,
48 2009). However, we have limited understanding of the frequency of flows worldwide or how often
49 they are triggered by specific mechanisms because their exact timing and character are often
50 problematic to measure. In most cases where a specific triggering mechanism has been identified, it
51 has been based on cable breaks or damage to other seafloor infrastructure (e.g. Hsu et al., 2008;
52 Cattaneo et al., 2012; see Talling et al., 2013 for more detail). This is particularly true of triggering of
53 sediment density flows by tropical cyclones (Bea et al., 1983; Dengler et al., 1984; Alvarado, 2006;
54 Carter et al., 2012; Gavey et al., 2016).

55 Using a global database of cable breaks, here we specifically focus on the role tropical cyclones play
56 in triggering damaging sediment density flows. Furthering previous spatially and temporally
57 restricted studies; the use of a global compilation of cable breaks allows the identification of areas
58 where damaging sediment density flows, triggered by cyclones occur and how frequent these events
59 have been globally over a 25 year time period.

60 **1.2. Aims**

61 Three main questions are addressed. First, how important are tropical cyclones for causing cable
62 breaks on a global basis, and in which settings (submarine canyons, etc.) and water depths do
63 cyclone induced breaks occur? Second, can the mechanisms by which cyclones trigger sediment
64 density flows be identified from cable breaks? For example, are flows triggered by storm waves and
65 currents during the tropical cyclone and/or are flows typically delayed and triggered a few days after
66 the passing of the tropical cyclone (Carter et al., 2012)? Third, is the frequency of cyclone-triggered
67 sediment density flows and cable breaks likely to change due to projected climate change?

68 **2. Data and methods**

69 **2.1. Cable break database**

70 This study is based on non-public, aggregated data supplied by Global Marine Systems Limited (UK)
71 on a non-disclosure basis. The database contains information on the location of each subsea cable
72 when it was laid (Fig. 1). It includes other installation information such as seabed type and duration
73 the cable has been in service. Cable breaks within the database are identified and generally related
74 to likely causes, i.e. seismic, trawling, anchor, etc. Each ‘break’ refers to a break or failure along a
75 section of a specific cable. A ‘break’ can range from internal damage of the power conductor or
76 optical fibres to the complete physical separation of the entire cable assembly. Each recorded
77 ‘break’ may therefore also represent multiple breaks along a single section of cable. The timing of a
78 break in the database is recorded to the nearest day.

79 **2.2. Tropical cyclone data**

80 **2.2.1. Tropical cyclone track data**

81 Historical tropical cyclone track data were obtained from the National Hurricane Center (NHC)
82 Hurdad-2 “best track” dataset (Landsea et al., 2013). This dataset is an archive compiled every 6
83 hours (at 0000, 0600, 1200, 1800 UTC) and includes reports of storm position and maximum wind
84 speeds.

85 **2.2.2. Tropical cyclone characterisation: ECMWF ERA-interim reanalysis data**

86 The global coverage of ocean buoys recording variables such as surface pressure and wave height is
87 spatially variable, and such data are not always freely available. The same is true of terrestrial
88 weather stations. Thus to analyse specific tropical cyclone characteristics we used global model data
89 in order to homogenise data quality. Records of tropical cyclone characteristics came from ERA-
90 Interim global atmospheric reanalysis produced by the European Centre for Medium-Range Weather
91 Forecasts (Dee et al., 2011). ERA-Interim covers the period from 1 January 1979 onwards, and
92 continues to be extended forward in near-real time. 3-hourly estimates of surface pressure (Pa),

93 significant wave height (m), total precipitation (m) and surface runoff (m) data were obtained from
94 the ERA-interim model. These data were gridded at a spatial resolution of $0.125^\circ \times 0.125^\circ$.

95 **2.3. Comparison of cable break and tropical cyclone databases**

96 All cable breaks within the database attributed to the following causes were included in our analysis:
97 earthquakes, landslides, chafe under current action, other natural causes, and unknown causes.
98 Among these categories, cable breaks with a known cause unrelated to tropical cyclones were
99 removed, such as those due to earthquakes (Pope et al., 2016). A tropical cyclone was attributed to
100 be the cause of a sediment density flow if the cable break coincided with the passing of a tropical
101 cyclone according to the best-track data and the ERA-interim data, or occurred within 14 days of the
102 end of a related river discharge peak if no other apparent triggers could be found.

103 Where a tropical cyclone appears to have triggered a sediment density flow, local environmental
104 variables were extracted from the ERA-Interim data. Where a cable break occurred beyond the
105 continental shelf edge, surface pressure and significant wave height measurements were measured
106 at the nearest point on the shelf edge. Where a cable break occurred on the shelf itself, surface
107 pressure and significant wave height were measured at the location of the cable break. Total
108 precipitation was measured at the nearest terrestrial location to each cable break; the maximum
109 distance was 260 km on the Mississippi Fan (mean distance of all the breaks; 95 km).

110 Breaks were attributed to by specific triggers depending on the timing of the break itself. A cable
111 break was specified as Type 1 if it occurred during the initial passing of the tropical cyclone and
112 coincided with rising or peaking significant wave heights, or a drop in surface pressure (Fig. 2). A
113 Type 2 cable break occurred after the peak in significant wave height, but coincident with the peak
114 in river flood discharges (Fig. 2). A Type 3 cable break followed the peak in cyclone-related river
115 flood discharge (Fig. 2). The time limit set for this was 14 days as a consequence of the variable flood
116 hydrographs, which can occur (Williams, 1969). Flood hydrographs can vary between different

117 basins as a consequence of the different shape and size of individual basins but also as a
118 consequence of differing relief and land-use patterns (Woods and Sivapalan, 1999). They can also
119 vary in shape in the same basin at different times according to different antecedent conditions. It
120 must also be acknowledged that as time between the hydrograph peak and the cable break
121 occurring increases, it become increasingly difficult to directly link the occurrence of a cable break to
122 the passage of the tropical cyclone rather than a separate mechanism. However, no obvious trigger,
123 such as an earthquake was observed in these cases.

124 **3. Results**

125 Globally, between January 1989 and January 2015, there were 35 cable breaks that could potentially
126 be attributed to tropical cyclone activity (Table 1). Cables broke in water depths of between 20 m
127 and 6120 m, of which 19 cables broke at water depths >2000 m. The largest number of breaks was
128 found offshore Taiwan; here 20 cable breaks were associated with tropical cyclones (Fig. 3a). There
129 were also 3 cable breaks off Japan and 1 off the Philippines (Fig. 3a). In the Indian Ocean, tropical
130 cyclone-related breaks were found offshore Madagascar (1 break) and La Reunion (6 breaks; Fig. 3b).
131 Elsewhere 3 breaks were found to have occurred in the Caribbean Sea and 1 break in the Eastern
132 Pacific (Fig. 3c).

133 The 35 cable breaks in the dataset were caused by 22 separate tropical cyclones. Multiple breaks
134 were caused by three tropical cyclones. Typhoon Sinlaku was the potential cause of 2 cable breaks
135 off East Taiwan in 2002. Cyclone Gamede was associated with 2 cable breaks offshore La Reunion in
136 2007. Typhoon Morakot resulted in 10 cable breaks. This number differs from previous studies of
137 Typhoon Morakot, which recorded “at least nine” cable breaks (Carter et al., 2012; Gavey et al.,
138 2016) as a consequence of additional data.

139 The 35 cable breaks potentially associated with tropical cyclones are found in several distinct
140 environmental settings (Table 1). The largest number of cable breaks (22) are found in or closely

141 associated with submarine canyons. Most of these are offshore Taiwan (19); others occurred
142 offshore the Philippines and Madagascar. The second most common location (9) for cable breaks is
143 close to river mouths or on associated deep-sea fans where turbidity currents are known to occur
144 (i.e. the Mississippi Fan, the Yellahs Fan). Of these, 6 are located within the sediment wave fields of
145 the Mafate and Saint-Denis Fans offshore La Reunion. The remainder of cable breaks (4) occurred on
146 open continental shelves and deep sea fans.

147 Assuming that each cable-breaking flow originated at the head of their associated submarine canyon
148 or at the mouth of close-by rivers, cables were broken at distances of between 1 and 384 km from
149 their source. The environmental settings of the cable breaks suggests that the majority of cable-
150 breaking sediment flows triggered by tropical cyclones began in areas where large volumes of
151 sediment had previously accumulated, such as in the heads of submarine canyons. They also suggest
152 that most damaging flows were channelized. Channelization likely increased the probability that the
153 flow would have sufficient power to break a cable, thus increasing the likelihood of detection in the
154 cable break database.

155 The timing of the 35 cable breaks relative to the passing of a tropical cyclone is highly variable (Table
156 1). Peaks in significant wave height and drops in surface pressure as the tropical cyclone passed
157 correspond to 4 cable breaks; each break was associated with an individual storm. Fig. 4 shows the
158 timing of a cable break coincident with the initial passing of Severe Tropical Storm Utor offshore
159 Taiwan in 2001. Tropical cyclone precipitation-related peaks in river discharge were associated with
160 13 cable breaks (Fig. 5). Both breaks associated with Cyclone Gamede were related to river
161 discharge. Most cable breaks (18) occurred following a delay from peak flood discharge of at least 2
162 days (Figs. 6 and 7). The longest delay was 12 days after river discharge had returned to pre-cyclone
163 levels (20 days after the peak discharge). Cable breaks associated with delays were associated with 9
164 tropical cyclones.

165 **4. Discussion**

166 **4.1. Tropical cyclone triggering of sediment density flows**

167 **4.1.1. Type 1 breaks: Direct and synchronous triggering of sediment density flows**

168 The cable break database shows that sediment density flows can be triggered (Type 1) during the
169 initial passing of a tropical cyclone (Figs. 4 and 7b). We attribute a Type 1 break to slope failure and
170 run-out triggered most likely by dynamic loading of the seafloor. Dynamic loading is the result of
171 storm waves, storm surges or internal waves occurring during a tropical cyclone (Prior et al., 1989;
172 Wright and Rathje, 2003). These breaks are attributed to dynamic loading-triggered sediment
173 density flows and not wave action alone because the breaks occur well below the wave base; at
174 depths greater than 1200 m (see Table 1). However, the lack of sequential breaks as seen in other
175 studies (Carter et al., 2012; Cattaneo et al., 2012; Gavey et al., 2016) means we cannot rule out other
176 causes.

177 Storm surges are generated by a combination of wind stresses and reduced atmospheric pressure
178 (Karim and Mimura, 2008). At the continental shelf edge, the advance of a storm surge can exert
179 large hydrodynamic pressures on the seafloor and elevate subsurface pore pressures (Zhang et al.,
180 2015). Such transient changes can promote slope instability and its run-out (Bea et al., 1983; Wright
181 and Rathje, 2003).

182 Storm waves can trigger sediment density flows through two processes. First, they can alter pore
183 pressures through dynamic loading. Passing wave crests increase pore pressures, while wave troughs
184 generate seepage pressures (Seed and Rahman, 1978). Where sediment lacks rigidity or has low
185 permeability, pore water pressures are able to progressively build or migrate laterally through the
186 sediment. Over time this can cause liquefaction or the rupture of inter-particle cohesive bonds (Puig
187 et al., 2008) leading to sediment failure (Lamb and Parsons, 2005). Second, the orbital motion of the
188 water particles can impart horizontal shear on the seabed (Jeng and Seymour, 2007). Where the
189 sediment shear strength is insufficient to resist the shear stress, failure and sediment transport can

190 occur in the form of plane shear, liquefied flow sliding or slope failure (Lambrechts et al., 2010).
191 Horizontal shear stresses induced by cyclone-forced currents can induce failure of weak sediments in
192 the same way (Alford, 2003).

193 The limited number (4 breaks) of Type 1 events compared to other break types suggests that
194 dynamic loading itself does not trigger large numbers of long run-out and damaging sediment
195 density flows. These processes are therefore likely to be more important for the entrainment and
196 deposition of shelf sediments (Sullivan et al., 2003). Failures of the deposited sediment may then
197 result from other triggers.

198 **4.1.2. Type 2 breaks: Indirect and near-synchronous triggering**

199 Type 2 cable breaks were three times more common (13 breaks) during the passage, or after the
200 peak of, a tropical cyclone, but after coincident peaks in wave height, surface pressure and rainfall
201 (Fig. 7c). Type 2 breaks are related to sediment density flows triggered by either cumulative effects
202 (rather than the peak event as in Type 1) of storm wave/current activity, or indirectly as a
203 consequence of peak river flood discharges resulting from tropical cyclone precipitation. Peak flood
204 discharges often coincide with continued storm wave activity; hence isolation of a specific
205 mechanism for Type 2 breaks is difficult from the cable break database alone. Typhoon Morakot (Fig.
206 5; Carter et al., 2012) is the best known example of a peak flood discharge trigger for a sediment
207 density flow that lagged behind the peak intensity of the cyclone itself. Sufficiently large flood
208 discharges can trigger sediment density flows either through the generation of hyperpycnal plumes
209 (Parsons et al., 2001; Mulder et al., 2003; Piper and Normark, 2009) or through rapid deposition and
210 subsequent remobilisation of river plume sediments (Parsons et al., 2001; Clare et al., 2016; Gavey
211 et al., 2016). In both cases the initial flow entrains water and sediment; thus giving the flow
212 sufficient energy to break a subsea cable (Fig. 7c).

213 **4.1.3. Type 3 breaks: Indirect and delayed triggering**

214 The largest number of cable breaks (18), occurred shortly after the passage of a tropical cyclone.
215 Here, we suggest that these Type 3 breaks relate to processes that lag behind the passage of a
216 tropical cyclone, but are still related to its residual effects (Figs 6 and 7d). Such lagged-triggering may
217 be related to the deposition of large volumes of sediment during and immediately after a storm.
218 Alternatively sediment at the shelf break or in canyon heads may have been destabilised by the
219 cumulative effects of surface gravity waves and internal tide/wave effects (Lee et al., 2009).

220 Storm wave/current action and flood discharges can transport and deposit large volumes of
221 sediment at the shelf edge or in canyon heads (Puig et al., 2004; Liu et al., 2009). The rate of
222 deposition may depend on; (1) the extent to which the water column on the continental shelf has
223 been stirred up by the passage of the cyclone (Sullivan et al., 2003) and; (2) the response and size of
224 the nearby river basin (Chen et al., 2012). These aspects can lead to delayed failures due to
225 oversteepening and loading by rapidly deposited sediment, and inhibited dissipation of excess pore
226 pressures (Clare et al., 2016; Figs 6 and 7d).

227 Liquefaction related to storm waves may also cause delayed failures. Laboratory and field tests
228 focussing on earthquake shaking have shown that soil liquefaction beneath silt laminae, beds or
229 lenses present in sand layers can lead to the generation of water film layers (Scott and Zuckerman,
230 1972; Kokusho and Kojima, 2002). These water films can persist for several days after an earthquake,
231 acting as sliding surfaces for delayed sediment failures (Özener et al., 2009). If storm waves cause
232 liquefaction of seafloor sediments by the processes outlined in Section 4.1.1, then it is possible for
233 water film layers to be generated. Delayed failures can subsequently occur following these water
234 film layers.

235 **4.1.4. Do delayed cable breaks result from other factors?**

236 We now consider whether delayed cable breaks result from either the time taken for a sediment
237 density flow to reach a cable or whether the flow is in fact triggered by a process unrelated to the
238 tropical cyclone.

239 The time taken for a flow to reach a cable and be recorded as a cable break has inflated the delay
240 times given. A significant number of cable breaks (12) were located more than 100 km from the
241 likely initiation point for sediment density flows. Given reasonable flow speeds (Carter et al., 2012;
242 Cattaneo et al., 2012; Gavey et al., 2016) and the distances between the likely point of initiation and
243 the cable break, a delay of up to 2 days (48 hours) is likely. The format of the cable break database
244 may contribute to this delay, as it only records the timing of each break to the nearest day.

245 Quantifying whether a cyclone triggered a sediment density flow following a long delay, i.e. more
246 than 7 days, is more difficult. Prior to this study, delayed triggering of sediment density flows was
247 observed in several locations (Hsu et al., 2008; Carter et al., 2012; Clare et al., 2016). These studies
248 identified delays between peak discharge and the occurrence of a flow of between a few hours to a
249 week. There are, however, no measurements of changing subsurface properties up until eventual
250 failure in these previous studies or in this study. It is therefore difficult to precisely define the point
251 at which deposited sediment will no longer fail as a consequence of cyclone forcing, and thus require
252 an additional trigger. This should be the subject of future studies.

253 **4.2. Will climate change make tropical cyclone triggered sediment density flows more likely?**

254 Understanding whether the frequency of cyclone-triggered sediment density flows will increase as a
255 consequence of climate change faces a number of challenges. First, possible trends in tropical
256 cyclone activity remain uncertain as a consequence of the short period of accurate observation and
257 the large amount of natural inter-annual variability (Knutson et al., 2010). This variability contributes
258 to uncertainty in predictive modelling of different warming scenarios (Sugi et al., 2009; Knutson et
259 al., 2010). Second, the number of fibre-optic cables and the diversity of cable locations have

260 increased due to growing reliance on this communications network (Carter et al., 2014; Pope et al.,
261 2016). These factors complicate the interpretation of whether changes to the number of observed
262 tropical cyclone triggered flows are a consequence of changes to tropical cyclone activity or to
263 hazard exposure of the cable network. It is therefore difficult to make projections of trends in the
264 number of cable breaks. One exception is the northwestern Pacific (Mei and Xie, 2016). Here,
265 increasing cyclone intensity (Emanuel, 2005), poleward migration of storm tracks (Kossin et al.,
266 2014) and slower tropical cyclone passage (Lee et al., 2015) have been linked to increased sediment
267 discharge to the continental shelf (Lee et al., 2015; Mei and Xie, 2016). The likelihood that cyclones
268 will trigger sediment density flows or at least precondition slopes to fail, triggered by other
269 processes (e.g. earthquakes; Gavey et al., 2016; Pope et al., 2016) is thereby enhanced. Increased
270 tropical cyclone activity does therefore appear to increase the likelihood of flow triggering.

271 **5. Conclusions**

272 Tropical cyclones trigger cable-breaking sediment density flows in almost all areas where cyclones
273 occur globally. Cyclone-forced flows are particularly common around South East Asia, especially off
274 Taiwan and the Philippines. Flows can be triggered by dynamic loading of the seabed through storm
275 surge and storm-wave action, but are more commonly the result of fluvial flood discharge.
276 Importantly, they are also triggered indirectly after a tropical cyclone has passed when large
277 volumes of rapidly deposited fluvial and shelf sediment are prone to failure. Such deposits may be
278 subject to delayed failure to form cable-damaging flows. It is unclear whether climate change will
279 affect the global frequency of tropical cyclone triggered flows, but it is likely to increase the number
280 of cable breaks in major cable corridors such as off Taiwan.

281 **Acknowledgements**

282 We are very grateful to Global Marine Systems Ltd. (GMSL) for access and permission to use its cable
283 break database. In this regard, the assistance of Brian Perrat and Steve Holden of GMSL is

284 particularly appreciated. General information on subsea telecommunications cables was generously
285 supplied by the International Cable Protection Committee and its members. We thank the British
286 Atmospheric Data Centre and ECMWF for providing reanalysis data. This work was supported by two
287 NERC Environmental Risks to Infrastructure Innovation Programme grants (NE/N012798/1 and
288 NE/P009190/1). Talling was supported by a NERC Royal Society Industry Fellowship to understand
289 submarine sediment flows and the risk they pose to global telecommunications. Clare was
290 supported by a NERC Knowledge Exchange Fellowship to identify and fill the gaps in knowledge of
291 environmental risks to infrastructure (NE/P005780/1). We would like to thank the editor Martin
292 Frank, David Piper and an anonymous reviewer for their in depth reviews and comments which
293 greatly improved this manuscript.

294

295

296

297

298 **References**

- 299 Alford, M.H., 2003. Redistribution of energy available for ocean mixing by long-range propagation of
300 internal waves. *Nature* 423, 159-162.
301
- 302 Alvarado, A., 2006. Updates on MMS (Minerals Management Service) regulatory issues for offshore
303 operators. Uniform Resource Locator (URL):
304 <http://www.southerngas.org/EVENTS/documents/SGAOGO06Alvarado.pdf> (accessed 13 March,
305 2007).
306
- 307 Bea, R.G., Wright, S.G., Sircar, P., Niedoroda, A.W., 1983. Wave-Induced Slides in South Pass Block
308 70, Mississippi Delta. *Journal of Geotechnical Engineering-Asce* 109, 619-644.
309
- 310 Becker, J.J., Sandwell, D.T., Smith, W.H.F., Braud, J., Binder, B., Depner, J., Fabre, D., Factor, J.,
311 Ingalls, S., Kim, S.H., 2009. Global bathymetry and elevation data at 30 arc seconds resolution:
312 SRTM30_PLUS. *Marine Geodesy* 32, 355-371.
313
- 314 Burnett, D.R., Beckman, R., Davenport, T.M., 2013. *Submarine Cables: the handbook of Law and*
315 *Policy*. Martinus Nijhoff Publishers.
316
- 317 Carter, L., Burnett, D., Drew, S., Hagadorn, L., Marle, G., Bertlett-McNeil, D., Irvine, N., 2009.
318 *Submarine cables and the oceans- connecting the world: UNEP-WCMC Biodiversity Series* 31.
319 *ICPC/UNEP/UNEP-WCMC*. 64.
320
- 321 Carter, L., Milliman, J.D., Talling, P.J., Gavey, R., Wynn, R.B., 2012. Near-synchronous and delayed
322 initiation of long run-out submarine sediment flows from a record-breaking river flood, offshore
323 Taiwan. *Geophysical Research Letters* 39.
324
- 325 Carter, L., Gavey, R., Talling, P.J., Liu, J.T., 2014. Insights into submarine geohazards from breaks in
326 subsea telecommunication cables. *Oceanography* 27, 58-67.
327
- 328 Cattaneo, A., Babonneau, N., Ratzov, G., Dan-Unterseh, G., Yelles, K., Bracene, R., De Lepinay, B.M.,
329 Boudiaf, A., Déverchère, J., 2012. Searching for the seafloor signature of the 21 May 2003
330 Boumerdes earthquake offshore central Algeria. *Natural Hazards and Earth System Sciences* 12,
331 2159-2172.
332
- 333 Chen, J.C., Huang, W.S., Jan, C.D., Yang, Y.H., 2012. Recent changes in the number of rainfall events
334 related to debris-flow occurrence in the Chenyulan Stream Watershed, Taiwan. *Natural Hazards and*
335 *Earth System Science* 12, 1539-1549.
336
- 337 Clare, M.A., Hughes Clarke, J.E., Talling, P.J., Cartigny, M.J.B., Pratomo, D.G., 2016. Preconditioning
338 and triggering of offshore slope failures and turbidity currents revealed by most detailed monitoring
339 yet at a fjord-head delta. *Earth and Planetary Science Letters* 450, 208-220.
340
- 341 Dee, D.P., Uppala, S.M., Simmons, A.J., Berrisford, P., Poli, P., Kobayashi, S., Andrae, U., Balmaseda,
342 M.A., Balsamo, G., Bauer, P., Bechtold, P., Beljaars, A.C.M., van de Berg, L., Bidlot, J., Bormann, N.,
343 Delsol, C., Dragani, R., Fuentes, M., Geer, A.J., Haimberger, L., Healy, S.B., Hersbach, H., Hólm, E.V.,
344 Isaksen, I., Kållberg, P., Köhler, M., Matricardi, M., McNally, A.P., Monge-Sanz, B.M., Morcrette, J.J.,
345 Park, B.K., Peubey, C., de Rosnay, P., Tavolato, C., Thépaut, J.N., Vitart, F., 2011. The ERA-Interim
346 reanalysis: configuration and performance of the data assimilation system. *Quarterly Journal of the*
347 *Royal Meteorological Society* 137, 553-597.

348
349 Dengler, A.T., Wilde, P., Noda, E.K., Normark, W.R., 1984. Turbidity currents generated by Hurricane
350 Iwa. *Geo-Marine Letters* 4, 5-11.
351
352 Emanuel, K., 2005. Increasing destructiveness of tropical cyclones over the past 30 years. *Nature*
353 436, 686-688.
354
355 Gavey, R., Carter, L., Liu, J.T., Talling, P.J., Hsu, R.T., Pope, E.L., Evans, G., 2016. Frequent sediment
356 density flows formed by different triggering mechanisms: observations from subsea cable breaks in
357 the Gaoping Canyon-Manila Trench, Taiwan. *Marine Geology*.
358
359 Hsu, S.K., Kuo, J., Lo, C.L., Tsai, C.H., Doo, W.B., Ku, C.Y., Sibuet, J.C., 2008. Turbidity Currents,
360 Submarine Landslides and the 2006 Pingtung Earthquake off SW Taiwan. *Terrestrial Atmospheric
361 and Oceanic Sciences* 19, 767-772.
362
363 Jeng, D.-S., Seymour, B.R., 2007. Simplified analytical approximation for pore-water pressure buildup
364 in marine sediments. *Journal of Waterway Port Coastal and Ocean Engineering-Asce* 133, 309-312.
365
366 Karim, M.F., Mimura, N., 2008. Impacts of climate change and sea-level rise on cyclonic storm surge
367 floods in Bangladesh. *Global Environmental Change* 18, 490-500.
368
369 Knutson, T.R., McBride, J.L., Chan, J., Emanuel, K., Holland, G., Landsea, C., Held, I., Kossin, J.P.,
370 Srivastava, A.K., Sugi, M., 2010. Tropical cyclones and climate change. *Nature Geoscience* 3, 157-163.
371
372 Kokusho, T., Kojima, T., 2002. Mechanism for postliquefaction water film generation in layered sand.
373 *Journal of geotechnical and geoenvironmental engineering* 128, 129-137.
374
375 Kossin, J.P., Emanuel, K.A., Vecchi, G.A., 2014. The poleward migration of the location of tropical
376 cyclone maximum intensity. *Nature* 509, 349-352.
377
378 Lamb, M.P., Parsons, J.D., 2005. High-density suspensions formed under waves. *Journal of
379 Sedimentary Research* 75, 386-397.
380
381 Lambrechts, J., Humphrey, C., McKinna, L., Gourage, O., Fabricius, K.E., Mehta, A.J., Lewis, S.,
382 Wolanski, E., 2010. Importance of wave-induced bed liquefaction in the fine sediment budget of
383 Cleveland Bay, Great Barrier Reef. *Estuarine, Coastal and Shelf Science* 89, 154-162.
384
385 Landsea, C., Franklin, J., Beven, J., 2013. The revised Atlantic hurricane database (HURDAT2). United
386 States National Oceanic and Atmospheric Administration's.
387
388 Lee, I.-H., Lien, R.-C., Liu, J.T., Chuang, W.S., 2009. Turbulent mixing and internal tides in Gaoping
389 (Kaoping) submarine canyon, Taiwan. *Journal of Marine Systems* 76, 383-396.
390
391 Lee, T.-Y., Huang, J.-C., Lee, J.-Y., Jien, S.-H., Zehetner, F., Kao, S.-J., 2015. Magnified Sediment Export
392 of Small Mountainous Rivers in Taiwan: Chain Reactions from Increased Rainfall Intensity under
393 Global Warming. *PloS one* 10, e0138283.
394
395 Liu, J.T., Hung, J.J., Lin, H.L., Huh, C.A., Lee, C.L., Hsu, R.T., Huang, Y.W., Chu, J.C., 2009. From
396 suspended particles to strata: The fate of terrestrial substances in the Gaoping (Kaoping) submarine
397 canyon. *Journal of Marine Systems* 76, 417-432.
398

399 Lu, J.Y., Hong, J.H., Su, C.C., Wang, C.Y., Lai, J.S., 2008. Field measurements and simulation of bridge
400 scour depth variations during floods. *Journal of Hydraulic Engineering* 134, 810-821.
401

402 Mei, W., Xie, S.P., 2016. Intensification of landfalling typhoons over the northwest Pacific since the
403 late 1970s. *Nature Geoscience* 9, 753-757.
404

405 Mulder, T., Syvitski, J.P.M., Migeon, S., Faugeres, J.-C., Savoye, B., 2003. Marine hyperpycnal flows:
406 initiation, behavior and related deposits. A review. *Marine and Petroleum Geology* 20, 861-882.
407

408 Özener, P.T., Özyayın, K., Berilgen, M.M., 2009. Investigation of liquefaction and pore water pressure
409 development in layered sands. *Bulletin of Earthquake Engineering* 7, 199-219.
410

411 Parsons, J.D., Bush, J.W.M., Syvitski, J.P.M., 2001. Hyperpycnal plume formation from riverine
412 outflows with small sediment concentrations. *Sedimentology* 48, 465-478.
413

414 Peduzzi, P., Chatenoux, B., Dao, H., De Bono, A., Herold, C., Kossin, J., Mouton, F., Nordbeck, O.,
415 2012. Global trends in tropical cyclone risk. *Nature Clim. Change* 2, 289-294.
416

417 Piper, D.J.W., Normark, W.R., 2009. Processes that initiate turbidity currents and their influence on
418 turbidites: a marine geology perspective. *Journal of Sedimentary Research* 79, 347-362.
419

420 Pope, E.L., Talling, P.J., Carter, L., 2016. Which earthquakes trigger damaging submarine mass
421 movements: Insights from a global record of submarine cable breaks? *Marine Geology*.
422

423 Prior, D.B., Suhayda, J.N., Lu, N.-Z., Bornhold, B.D., Keller, G.H., Wiseman, W.J., Wright, L.D., Yang, Z.-
424 S., 1989. Storm wave reactivation of a submarine landslide. *Nature* 341, 47-50.
425

426 Puig, P., Ogston, A.S., Mullenbach, B.L., Nittrouer, C.A., Parsons, J.D., Sternberg, R.W., 2004. Storm-
427 induced sediment gravity flows at the head of the Eel submarine canyon, northern California margin.
428 *Journal of Geophysical Research: Oceans* 109.
429

430 Puig, P., Palanques, A., Orange, D.L., Lastras, G., Canals, M., 2008. Dense shelf water cascades and
431 sedimentary furrow formation in the Cap de Creus Canyon, northwestern Mediterranean Sea.
432 *Continental Shelf Research* 28, 2017-2030.
433

434 Scott, R.F., Zuckerman, K.A., 1972. Sandblows and liquefaction in the great Alaska earthquake of
435 1964. *Engineering Publication* 1606, 170-189.
436

437 Seed, H.B., Rahman, M.S., 1978. Wave-induced pore pressure in relation to ocean floor stability of
438 cohesionless soils. *Marine Georesources & Geotechnology* 3, 123-150.
439

440 Stocker, T.F., 2014. *Climate change 2013: the physical science basis: Working Group I contribution to
441 the Fifth assessment report of the Intergovernmental Panel on Climate Change*. Cambridge
442 University Press.
443

444 Sugi, M., Murakami, H., Yoshimura, J., 2009. A reduction in global tropical cyclone frequency due to
445 global warming. *Sola* 5, 164-167.
446

447 Sullivan, M.C., Cowen, R.K., Able, K.W., Fahay, M.P., 2003. Effects of anthropogenic and natural
448 disturbance on a recently settled continental shelf flatfish. *Marine Ecology Progress Series* 260, 237-
449 253.

450

451 Talling, P.J., Paull, C.K., Piper, D.J.W., 2013. How are subaqueous sediment density flows triggered,
452 what is their internal structure and how does it evolve? Direct observations from monitoring of
453 active flows. *Earth-Science Reviews* 125, 244-287.

454

455 Williams, J.R., 1969. Flood routing with variable travel time or variable storage coefficients.
456 *Transactions of the ASAE* 12, 100-0103.

457

458 Woods, R., Sivapalan, M., 1999. A synthesis of space-time variability in storm response: Rainfall,
459 runoff generation, and routing. *Water Resources Research* 35, 2469-2485.

460

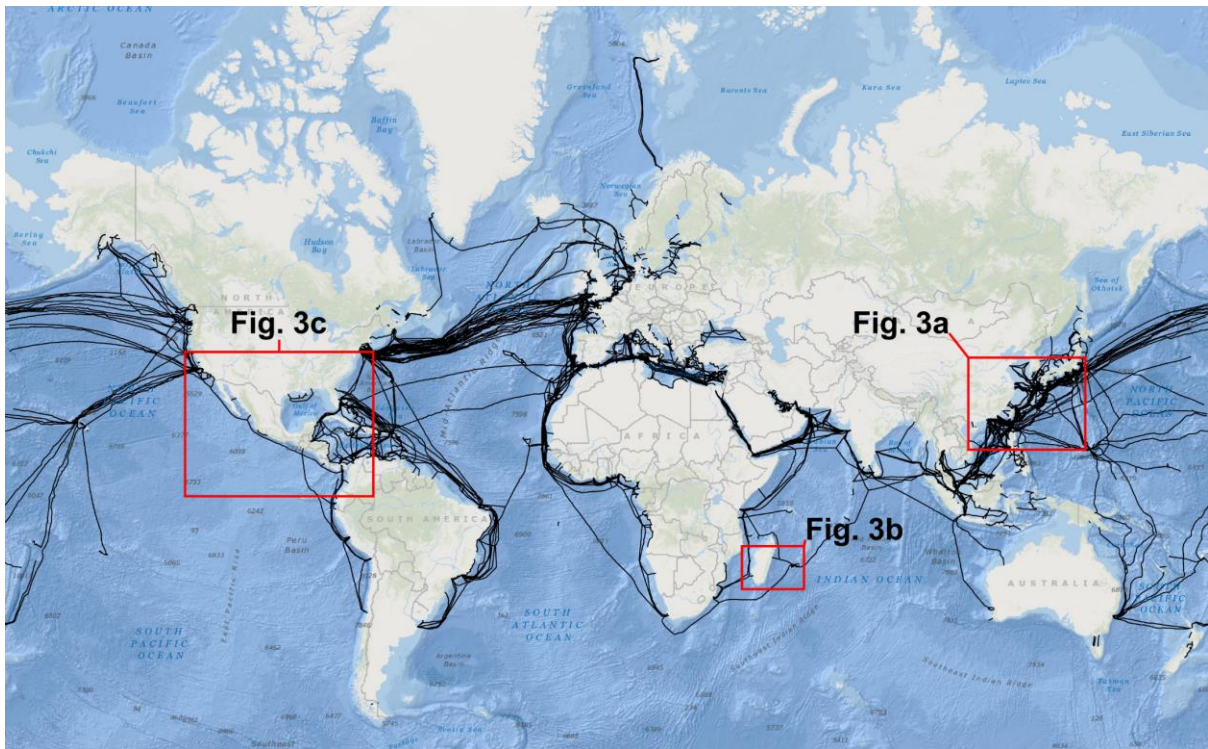
461 Wright, S.G., Rathje, E.M., 2003. Triggering mechanisms of slope instability and their relationship to
462 earthquakes and tsunamis. *Pure and Applied Geophysics* 160, 1865-1877.

463

464 Zhang, M., Huang, Y., Bao, Y., 2015. The mechanism of shallow submarine landslides triggered by
465 storm surge. *Natural Hazards*, 1-11.

466

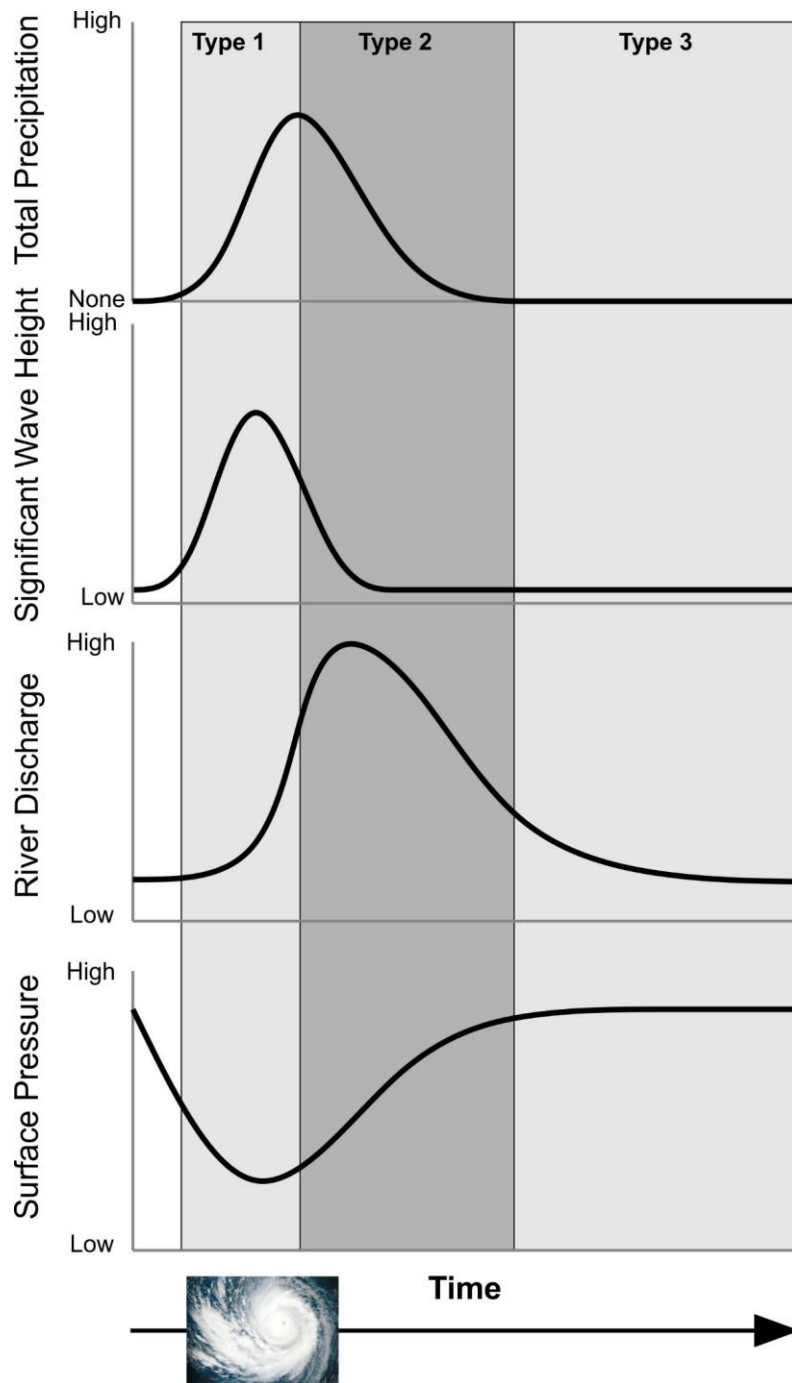
467



469

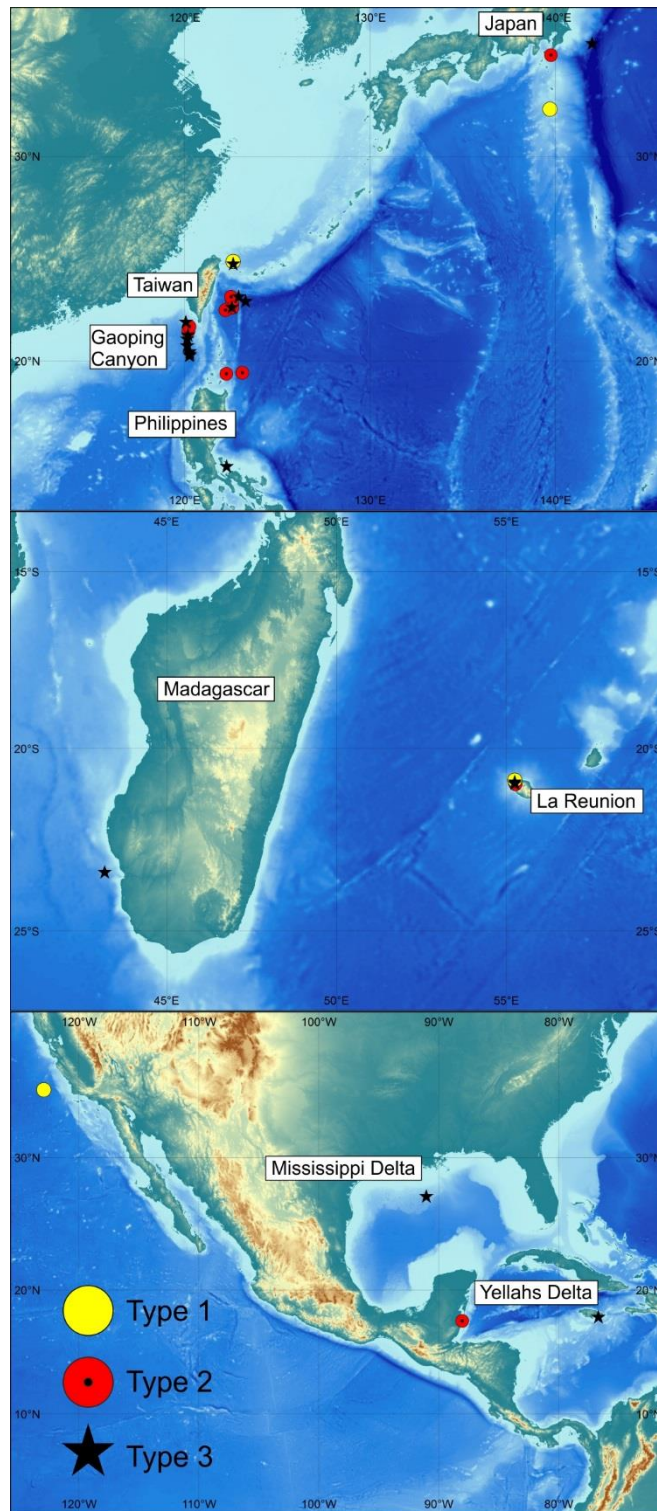
470 Fig. 1. Map of the submarine cable network used in this study.

471



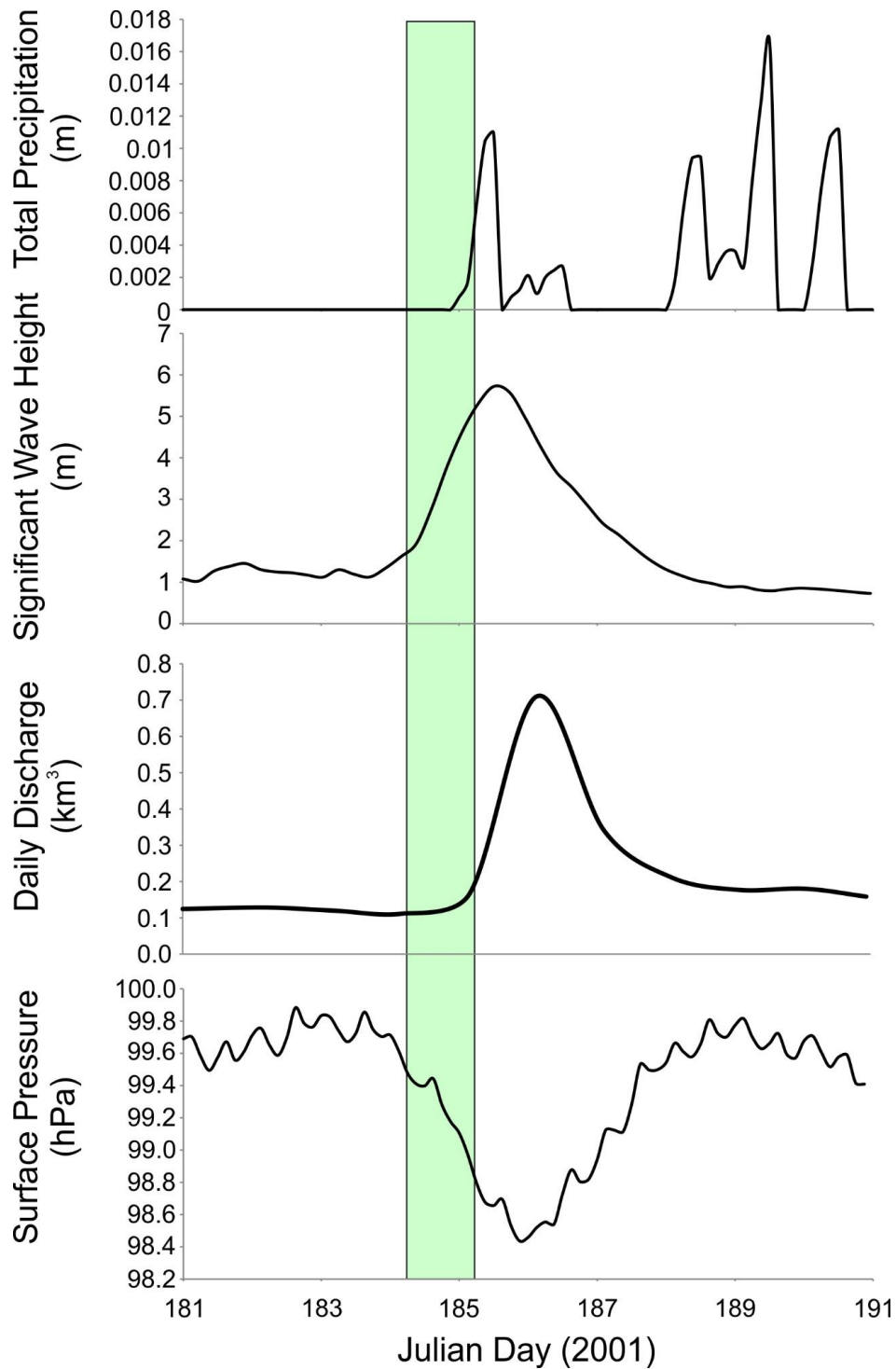
472

473 Fig. 2. Idealised schematic of the relationship between environmental variables during the passage
 474 of a tropical cyclone and the timing of a cable break. Type 1 breaks are defined as occurring with
 475 rising and peaking significant wave heights and storm driven flows or the drop in surface pressure
 476 associated with the passage of a tropical cyclone. Type 2 occur after the peak in significant wave
 477 height but associated with the peak in river flood discharges. Type 3 occur if the break was within 14
 478 days of the peak in cyclone related river flood discharge.



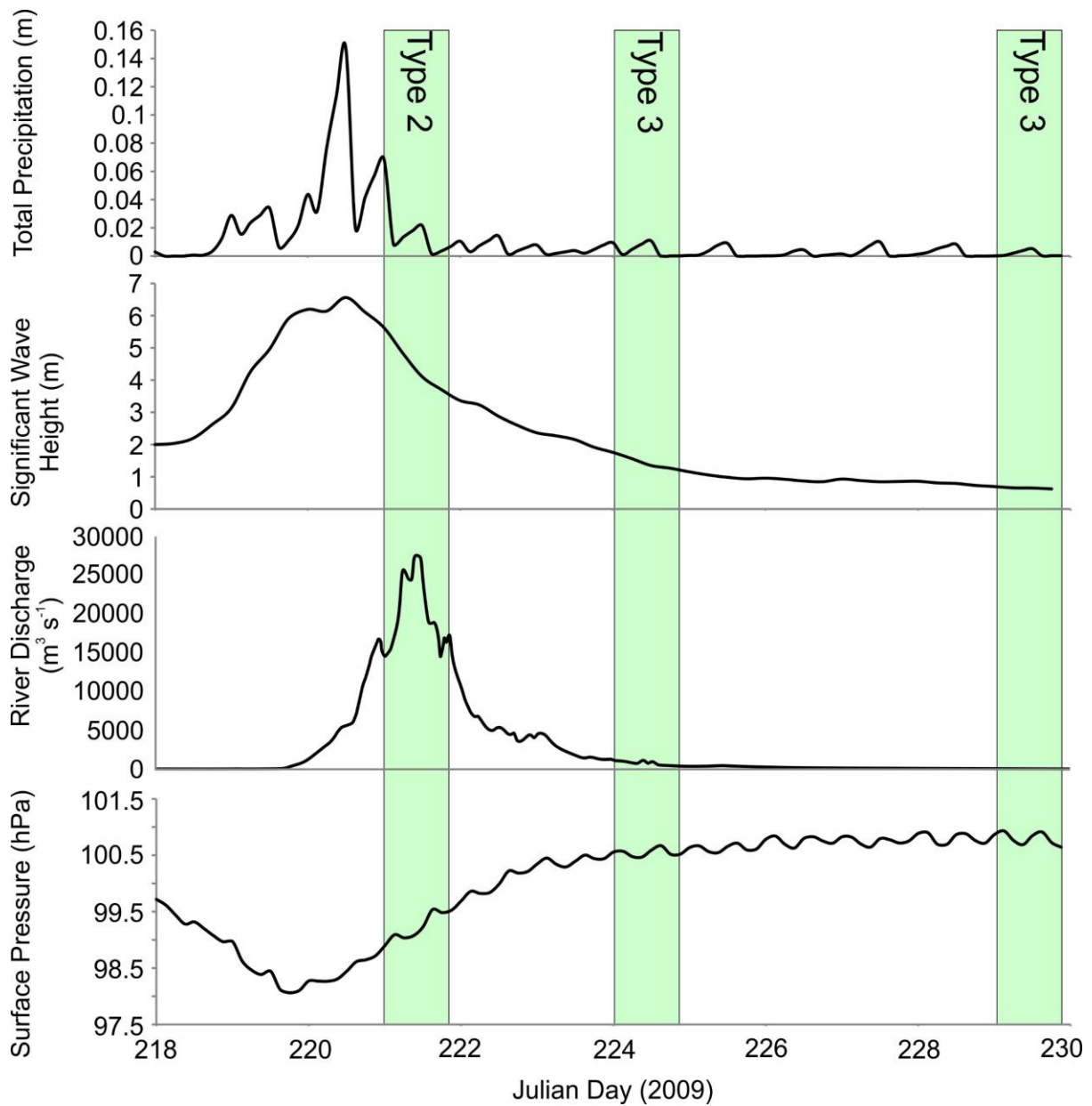
479

480 Fig. 3. Locations of submarine cable breaks inferred to be associated with tropical cyclones. a) Cable
 481 breaks offshore Japan, Taiwan and the Philippines. b) Cable breaks offshore Madagascar and La
 482 Reunion. c) Cable breaks offshore the USA, Central America and the Caribbean Islands. Bathymetry
 483 and topographic data were obtained from the GEBCO database (Becker et al., 2009).



484

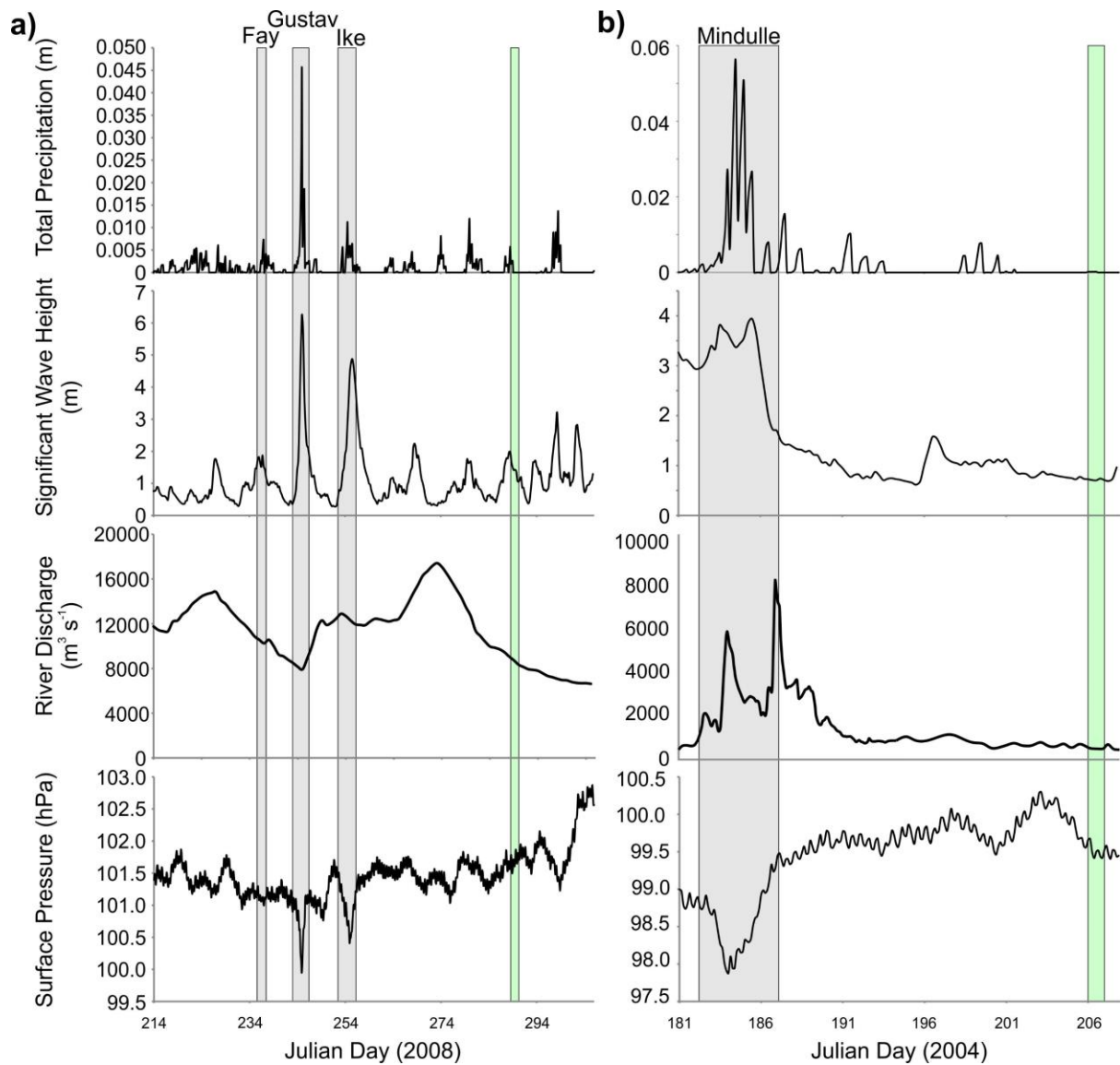
485 Fig. 4. An example of a Type 1 cable break that is synchronous with typhoon induced wave height
 486 increases. Changes in rainfall, wave height and surface air pressure during a tropical cyclone and the
 487 relative timing of cable breaks offshore Taiwan in 2001. ERA-Interim data for the cable break
 488 occurring offshore Taiwan during the passage of Severe Storm Utor, 2001. Green bar represents the
 489 time when the cable broke.



490

491 Fig. 5. An example of Type 2 and 3 cable breaks. Environmental conditions for cable breaks occurring
 492 at the peak flood discharge resulting from the passing of a tropical cyclone. ERA-Interim data for
 493 total precipitation, significant wave height and surface pressure displayed are for offshore Taiwan at
 494 the head of the Gaoping Canyon for Typhoon Morakot in 2009. River discharge for the Gaoping River
 495 during Typhoon Morakot is also displayed (Carter et al., 2012). Green bars represent the time when
 496 cables were broken. The first set of cable breaks represents a Type 2 break. The second and third
 497 sets of cable breaks represent Type 3 breaks.

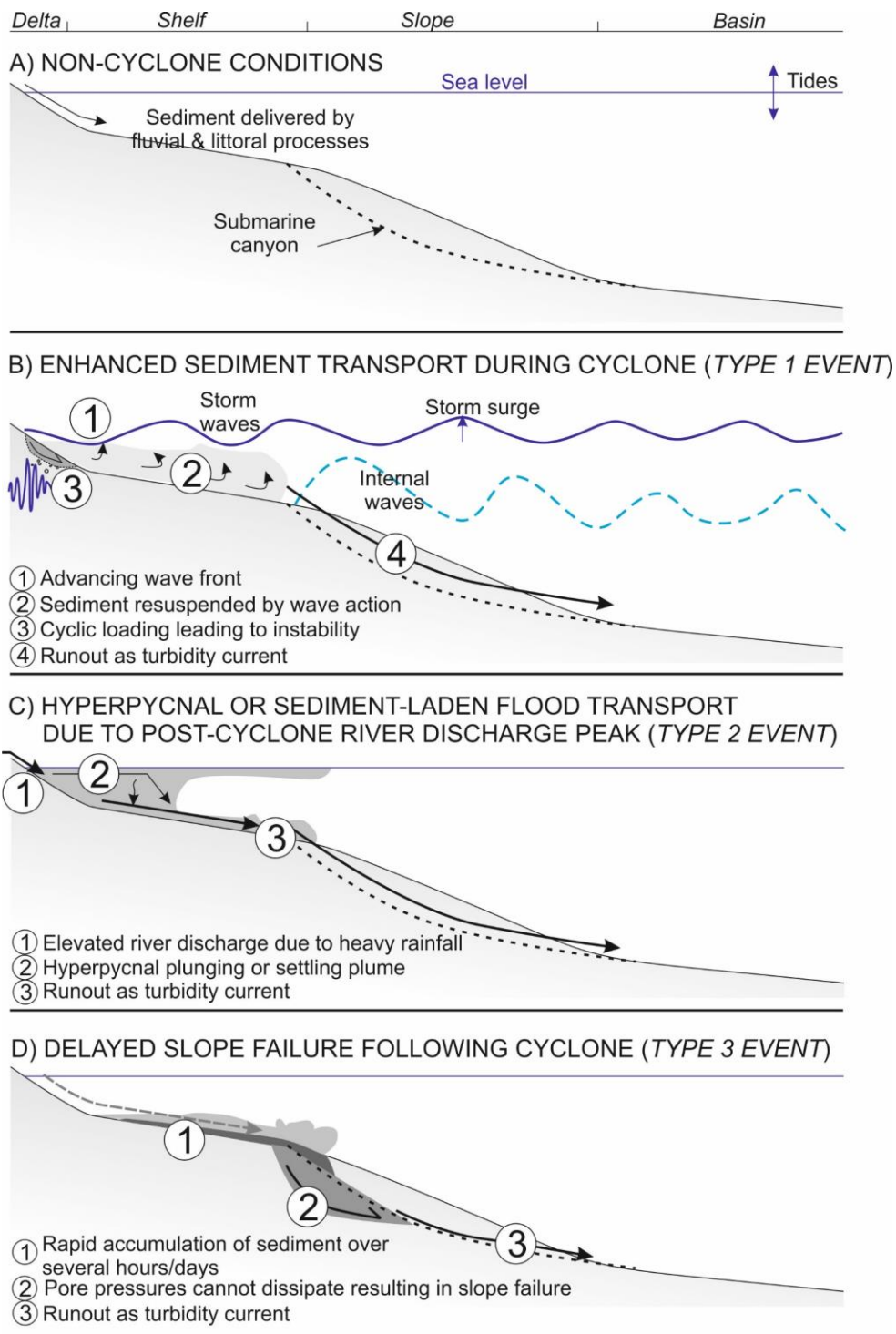
498



499

500 Fig. 6. Examples of Type 3 breaks. Environmental conditions for cable breaks occurring after the
 501 reduction in peak flood discharge following the passing of a tropical cyclone. a) ERA-Interim data for
 502 total precipitation, significant wave height and surface pressure displayed are for the Mississippi
 503 Delta following the passing of Tropical Storm Fay, Hurricane Gustav and Hurricane Ike in 2008. River
 504 discharge data is from a river station at Baton Rouge on the Mississippi. b) ERA-interim data for total
 505 precipitation, significant wave height and surface pressure displayed are for Taiwan following the
 506 passing of Typhoon Mindulle in 2004. River discharge data is from the Choshui River (Lu et al., 2008).
 507 Green bar represents the time when the cable break occurred.

508



509

510 Fig. 7. Illustration of the various hypotheses for the triggering of sediment density flows during and
 511 after cyclones. a) Sediment delivery and transport during non-tropical cyclone conditions. b) Type 1
 512 event triggering mechanisms. c) Type 2 event triggering mechanisms. d) Type 3 event triggering
 513 mechanisms.

Location	Water Depth (m)	Date	Setting	Distance from likely source (km)	Relative Timing	Related Tropical Cyclone	Interpreted Type
Izu-Bonin Ridge	1560	15/06/2005	Continental slope (Possible sediment wave field)	36	Significant wave height peak	Typhoon Nesat	Type 1
La Reunion	1214	19/02/2006	Mafate and Saint-Denis Fans	13	Significant wave height peak Surface pressure trough	Severe Tropical Storm 9	Type 1
Taiwan Pacific	1518	03/07/2001	Chilung Canyon	78	Significant wave height rising limb	Severe Tropical Storm Utori	Type 1
North America	4100	13/09/2000	Deep sea fan	185	Surface Pressure Trough	Hurricane Lane	Type 1
Belize	20	01/11/2011	Open continental shelf	16	Peak runoff	Hurricane Rina	Type 2
Japan	2000	25/09/1996	Boso Canyon	98	Peak discharge	Typhoon Violet	Type 2
La Reunion	903	02/03/2007	Mafate and Saint-Denis Fans	9	Peak discharge	Cyclone Gamede	Type 2
La Reunion		03/03/2007	Mafate and Saint-Denis Fans	10	Peak discharge	Cyclone Gamede	Type 2
La Reunion		04/10/2008	Mafate and Saint-Denis Fans	1	Peak discharge	Zone of disturbed weather	Type 2
Philippines	4646	07/10/1993	Cagayan Canyon	210	Falling limb of peak discharge	Typhoon Kadiang	Type 2
Philippines	1683	07/12/2004	Cagayan Canyon	140	Falling limb of peak discharge	Typhoon Nanmadol	Type 2
Taiwan	5700	12/09/2002	Taitung Canyon	213	Rising limb of peak discharge	Typhoon Sinlaku	Type 2
Taiwan	5500	21/08/2007	Haulien Canyon	126	Peak discharge	Typhoon Sepat	Type 2
Taiwan	5200	28/07/2014	Taitung Canyon	187	Rising limb of peak discharge	Typhoon Matmo	Type 3
Taiwan	2876	09/08/2009	Gaoping Canyon	157	Falling limb of peak discharge	Typhoon Morakot	Type 2
Taiwan	1992	09/08/2009	Gaoping Canyon	117	Falling limb of peak discharge	Typhoon Morakot	Type 2
Taiwan	4440	09/08/2009	Taitung Canyon	145	Falling limb of peak discharge	Typhoon Morakot	Type 2
Jamaica	996	21/09/2004	Yellahs Fan	7	1 after peak discharge	Hurricane Ivan	Type 3
Japan	6120	07/10/2007	Mogi Fan	129	10 days after peak discharge	Typhoon Krosa	Type 3
La Reunion	550	16/02/2009	Mafate and Saint-Denis Fans	9	7 days after peak discharge	Typhoon Gael	Type 3
La Reunion	820	28/10/2006	Mafate and Saint-Denis Fans	4	10 days after peak discharge	Tropical Disturbance 1	Type 3
Madagascar	2897	12/03/2011	Onilahy Canyon	64	14 days after peak discharge	Cyclone Bingiza	Type 3
Mississippi	1541	15/10/2008	Mississippi Fan	104	17 days after peak discharge	Hurricanes Fay, Gustav, Ike	Type 3
Philippines	77	30/12/1994	Continental Shelf	40	7 days after peak discharge	Typhoon Axel	Type 3
Taiwan	6024	21/09/2002	Haulien Canyon	135	11 days after peak discharge	Typhoon Sinlaku	Type 3
Taiwan	6000	18/11/2003	Haulien Canyon	170	8 days after peak discharge	Typhoon Melor	Type 3
Taiwan	1516	24/07/2004	Chilung Canyon	73	20 days after peak discharge	Typhoon Mindulle	Type 3
Taiwan	3990	12/08/2009	Gaoping Canyon	384	4 days after peak discharge	Typhoon Morakot	Type 3
Taiwan	4025	12/08/2009	Gaoping Canyon	364	4 days after peak discharge	Typhoon Morakot	Type 3
Taiwan	2646	12/08/2009	Gaoping Canyon	260	4 days after peak discharge	Typhoon Morakot	Type 3
Taiwan	1304	12/08/2009	Gaoping Canyon	110	4 days after peak discharge	Typhoon Morakot	Type 3
Taiwan	3816	13/08/2009	Gaoping Canyon	320	4 days after peak discharge	Typhoon Morakot	Type 3
Taiwan	3800	12/08/2009	Gaoping Canyon	355	4 days after peak discharge	Typhoon Morakot	Type 3
Taiwan	2800	12/08/2009	Gaoping Canyon	218	4 days after peak discharge	Typhoon Morakot	Type 3
Taiwan	5200	17/08/2009	Taitung canyon	170	9 days after peak discharge	Typhoon Morakot	Type 3

515

516 Table 1. Tropical cyclone triggered cable breaks. Depending on setting, the distance from likely
 517 source is defined as the approximate distance between the cable break and the canyon head, the
 518 river mouth or the shelf edge in the case of those occurring on the continental slope.